Lariat-Type B_{12} Model Complexes. 2. Ligand-Responsive NMR Trends of Pendant Methylpyridyl Costa-Type Organocobalt Complexes

Luigi G. Marzilli,* Alessandra Gerli, and Antonia M. Calafat

Department of Chemistry, Emory University, Atlanta, Georgia 30322

Received February 13, 1992

Recently prepared B_{12} model compounds [R(or X)Co(C_1py)]$^+$ were characterized in $CDCl_3$, DMSO-d_6, and CD_3-CN using 1D and modern 2D NMR methods. C_1py is the quinquedentate ligand 2,3,9,10-tetramethyl-6-(2-pyridylmethyl)-1,4,8,11-tetraazaundeca-1,3,8,10-tetraene-1,11-diolo. The pyridine moiety of C_1py is attached covalently at the 2-position by a one-methylene link to the central C of the propylene chain of (DO)(DOH)pn (N^2,$N^{2\prime}$-propanediylbis(2,3-butanedione 2-imine 3-oxime). Previous crystallographic studies demonstrated that the one-methylene link in C_1py derivatives allows coordination of the pyridine. In the present study, ^{1}H and ^{13}C NMR spectroscopy (including NOESY, HMQC, and HMBC) demonstrated coordination of the pendant pyridine in C_1py complexes even for [RCo(C_1py)]$^+$ in DMSO-d_6. For [R(or X)Co(C_1py)]ClO_4 compounds, the axial ^{1}H NMR signals shifted in the opposite direction to those of equatorial ^{1}H signals as R or X was changed. This pattern of ligand-responsive shift changes ($\Delta\delta_{LR}$) indicates that ^{1}H NMR shift changes are influenced primarily by cobalt anisotropy. ^{13}C NMR shifts of the pyridine γ-C correlate well with those of other B_{12} models and reflect the expected ability of R or X to donate electron density to cobalt. ^{13}C resonances of (a) pyridine carbons, (b) unsaturated conjugated carbons of the equatorial ligand macrocycle, and (c) the methyl carbons directly connected and coplanar with the conjugated system shift downfield as the electron donor ability of R (or X) is decreased. These results indicate that the $\Delta\delta_{LR}$ for these ^{13}C resonances are mainly sensitive to through-bond inductive effects. However, ^{13}C resonances of the saturated equatorial carbon in the middle of the propylene bridge (C6) shifted upfield as the donor ability of R (or X) decreased. This $\Delta\delta_{LR}$ trend for C6 cannot be explained by either inductive or anisotropic effects. A possible explanation for this effect is that the shift for C6 is influenced by strain in the linker arm caused by ligand-induced changes in Co–N axial bond lengths. This explanation was invoked earlier to interpret ^{31}P $\Delta\delta_{LR}$ for the linker arm of B_{12} compounds. In previous work, the magnitude of the downfield shift of the γ- and β-C's of pyridine on coordination has been associated with the extent of electron donation from the pyridine to the cobalt. The average magnitude of this coordination shift for [pyCo((DO)(DOH)pn)R]$^+$ complexes was less than that for [RCo(C_1py)]$^+$ complexes when the shifts, in this case, were compared to those of free 2-picoline. This result suggests greater electron donation by the pyridyl in C_1py compounds, consistent with the reported cathodic shift of the Co(III)/Co(II) redox potential in C_1py derivatives relative to analogous (DO)(DOH)pn derivatives. The differences in E_{pc} (the cathodic peak potential) for the analogues can be attributed to the one-methylene link that holds the pyridyl in C_1py derivatives in a position that allows a slightly shorter axial Co–N bond distance than in (DO)(DOH)pn derivatives. The Co(III)/Co(II) redox couple of the C_1py derivatives has been shown previously to correlate well with those of analogous B_{12} derivatives. Our analysis of $\Delta\delta_{LR}$ for equatorial C's suggests that the E_{pc} values do reflect the electronic properties of the Co center, at least in large part. However, more positive $E_{1/2}$ values have been reported for RB_{12} derivatives with R = bulky alkyl groups than for methyl-B_{12}. This relationship was attributed previously to weaker donation resulting from longer Co–C bonds for the bulky R groups, since otherwise the longer alkyl chains should make the larger groups better donors. However, our analysis of $\Delta\delta_{LR}$ of pyridyl C's of C_1py derivatives shows that the bulky R groups are better donors than methyl. The anodic shift of the derivatives with bulky alkyl groups can be attributed, instead, to the lower donation by the trans axial N-donor ligand. This explanation probably also applies to B_{12} compounds.

Introduction

In protein-mediated processes, the cobalt center of adenosylcobalamin (coenzyme B_{12}) provides a 5′-deoxyadenosyl radical via Co–C homolysis, but the factors that promote the facile Co–C bond cleavage in the protein-bound cofactor are still unknown.[1-4] Enzyme-induced conformational changes are almost certainly responsible for promoting cleavage.[1-6] Stabilization of the homolysis fragments by strong binding to the protein probably also plays a role.[7]

In the absence of a crystal structure of a holoenzyme, NMR spectroscopy appears to be the most promising means to investigate cobalamin structural/conformational changes in holoenzymes.[8-18] However, because of the sparse relevant structural information

(1) Halpern, J. *Science* **1985**, *227*, 869–875.
(2) Finke, R. G. In *Molecular Mechanisms in Bioorganic Processes*; Bleasdale, C., Golding, B. T., Eds.; The Royal Society: Cambridge, U.K., 1990; p 244.
(3) Finke, R. G.; Schiraldi, D. A.; Mayer, B. J. *Coord. Chem. Rev.* **1984**, *54*, 1–22.
(4) Marzilli, L. G. In *Bioinorganic Catalysis*; Reedijk, J., Ed.; Marcel Dekker: New York, 1992.
(5) Bresciani-Pahor, N.; Forcolin, M.; Marzilli, L. G.; Randaccio; Summers, M. F.; Toscano, P. J. *Coord. Chem. Rev.* **1985**, *63*, 1–125 and references therein.
(6) Randaccio, L.; Bresciani-Pahor, N.; Zangrando, E.; Marzilli, L. G. *Chem. Soc. Rev.* **1989**, *18*, 225–250.
(7) Krautler, B.; Keller, W.; Kratky, C. *J. Am. Chem. Soc.* **1989**, *111*, 8936–8938.
(8) Summers, M. F.; Marzilli, L. G.; Bax, A. *J. Am. Chem. Soc.* **1986**, *108*, 4285–4294.
(9) Bax, A.; Marzilli, L. G.; Summers, M. F. *J. Am. Chem. Soc.* **1987**, *109*, 566–574.
(10) Pagano, T. G.; Yohannes, P. G.; Hay, B. P.; Scott, J. R.; Finke, R. G.; Marzilli, L. G. *J. Am. Chem. Soc.* **1989**, *111*, 1484–1491.
(11) Pagano, T. G.; Marzilli, L. G.; Flocco, M. M.; Tsai, C.; Carrell, H. L.; Glusker, J. P. *J. Am. Chem. Soc.* **1991**, *113*, 531–542.
(12) Alelyunas, Y. W.; Fleming, P. E.; Finke, R. G.; Pagano, T. G.; Marzilli, L. G. *J. Am. Chem. Soc.* **1991**, *113*, 3781–3794.

0020-1669/92/1331-4617$03.00/0

on cobalamins,[11,13] studies aimed at identifying well-defined relationships between structure and spectroscopic properties have been carried out almost exclusively on simple model compounds.[5,19-31] The B_{12} NMR studies have involved primarily alkyl- or cyano-B_{12} derivatives.[8-18]

An important approach to these problems has been to assess the response of the shift (δ) of a given signal to changes in the R or X ligand. For some time, we have been interested in investigating such trends in ligand-responsive NMR chemical shift changes ($\Delta\delta_{LR}$) for simple model compounds.[5,19-31] Model compounds have the advantage that precise structural information can be obtained and that the diversity of axial ligands is greater than that for cobalamins. An understanding of the factors influencing $\Delta\delta_{LR}$ in simple compounds can facilitate the interpretation of spectral trends in the more complicated cobalamins. Studies with models have identified Co anisotropy, ($\Delta\chi$)[25,27] equatorial ligand anisotropy,[21,23] and inductive through-bond effects[26,29] as influencing $\Delta\delta_{LR}$ (for a review see ref 5). However, we were not able to assess quantitatively the relative contribution of inductive and dipolar effects on the ^1H and ^{13}C $\Delta\delta_{LR}$.[22-26] These effects most likely reflect ligand-responsive changes in Co electronic properties.

Our most recent investigations have focused on traditional Costa-type model compounds ([LCo((DO)(DOH)pn)R]X[21,22] and [LCo((DO)(DOH)Me_2pn)R]X[23] where (DO)(DOH)pn is the equatorial ligand $N^2,N^{2'}$-propanediylbis(2,3-butanedione 2-imine 3-oxime) (Figure 1) and (DO)(DOH)Me_2pn is a (DO)(DOH)pn-type equatorial ligand containing a 2,2-dimethylpropylene bridge). In these Costa-type and other types of models the anisotropic contribution of the equatorial ligand is not uniform in the equatorial plane. Furthermore, rotation of L around the Co–L bond leads to a family of conformations whose distribution may depend on various factors (e.g., bulk or electronic effect of R, solvent, etc.). Also, in Costa-type complexes, the anionic axial ligands have until recently been limited primarily to alkyl groups; derivatives with inorganic ligands have only recently been well characterized.[32] In both the long-known organocobalt and the new inorganic Costa-type species, axial ligands are readily displaced, complicating NMR studies.[32]

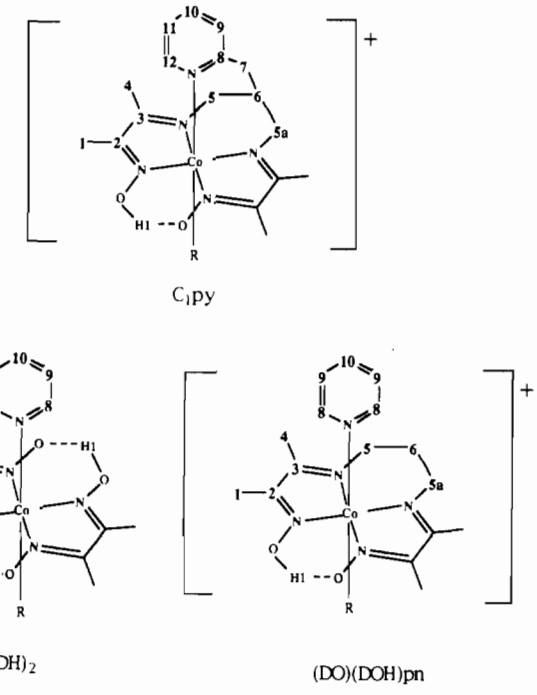

Figure 1. Structures of C_1py, (DO)(DOH)pn, and $(DH)_2$ (cobaloximes) derivatives with the atom-numbering schemes.

In order to overcome these limitations we have recently synthesized a new B_{12} model system that combines the corrin-like features of the Costa-type derivatives with an appended axial base (Figure 1).[33] The ligand in these new B_{12} model complexes, $[R(or X)Co(C_1py)]^+$, is unusual for a macrocycle with a pendant ligand since it is symmetrical, thus simplifying the NMR studies. Interpreting spectral and structural trends in such a rigid system may prove useful in assessing conformational and structural changes that lead to Co–C bond homolysis of coenzyme B_{12}. However, we needed to establish that the pendant pyridine was coordinated and to assign the signals unambiguously. Therefore, we used a battery of modern 2D NMR methods to achieve these goals.

In this report we examine ligand-responsive ^1H and ^{13}C NMR chemical shift trends for $[R(or X)Co(C_1py)]ClO_4$ compounds as R(or X) are changed. The axial ligand effects for these complexes are also compared with those for models with $(DH)_2$ (cobaloximes) (Figure 1) and (DO)(DOH)pn equatorial ligands. Since the ^{13}C shifts depend, in part, on the electronic properties of the metal center, these results can then be compared to electrochemical trends for C_1py derivatives. Such a comparison is meritorious since there is a close relationship between the redox properties of C_1py and B_{12} derivatives.[33]

Experimental Section

$[R(or X)Co(C_1py)]ClO_4$. Syntheses of these compounds, except where X = DMSO, have been described.[33] $[DMSOCo(C_1py)]^{2+}$ was prepared in situ for NMR study. To a solution of $[BrCo(C_1py)]ClO_4$ (0.0503 g, 0.1 mmol) in 1 mL of DMSO-d_6 was added $AgNO_3$ (0.0169 g, 0.01 mmol). The solution, protected from light, was stirred for 24 h and then filtered.

NMR Spectroscopy. ^1H and ^{13}C NMR spectra were recorded on a GE QE-300 spectrometer. All 2D NMR experiments were performed on a GE GN-500 spectrometer at 25 °C without sample spinning. Exact chemical shifts for all ^1H and ^{13}C resonances were obtained from the 1D spectra. Chemical shifts of the cobalt complexes (0.1 M) in $CDCl_3$, DMSO-d_6, or CD_3CN were referenced to internal Me_4Si.

NOESY Spectroscopy.[34] NOESY spectra of $[CH_3Co(C_1py)]ClO_4$ in CD_3CN and DMSO-d_6 resulted from a 1024 × 2048 data matrix size with 16 scans (preceded by 4 dummy scans (DS)) per t_1 value. The delay

(13) Rossi, M.; Glusker, J. P.; Randaccio, L.; Summers, M. F.; Toscano, P. J.; Marzilli, L. G. *J. Am. Chem. Soc.* **1985**, *107*, 1729–1738.
(14) Bratt, G. T.; Hogenkamp, H. P. C. *Biochemistry* **1984**, *23*, 5653–5659.
(15) Brown, K. L. *J. Am. Chem. Soc.* **1987**, *109*, 2277–2284.
(16) Brown, K. L.; Hakimi, J. M. *J. Am. Chem. Soc.* **1986**, *108*, 496–503.
(17) Brown, K. L.; Brooks, H. B.; Zou, X.; Victor, M.; Ray, A.; Timkovich, R. *Inorg. Chem.* **1990**, *29*, 4844–4846.
(18) Brown, K. L.; Brooks, H. B.; Gupta, B. D.; Victor, M.; Marques, H. M.; Scooby, D. C.; Goux, W. J.; Timkovich, R. *Inorg. Chem.* **1991**, *30*, 3430–3438.
(19) Zangrando, E.; Bresciani-Pahor, N.; Randaccio, L.; Charland, J.-P.; Marzilli, L. G. *Organometallics* **1986**, *5*, 1938–1944.
(20) Marzilli, L. G.; Bayo, F.; Summers, M. F.; Thomas, L. B.; Zangrando, E.; Bresciani-Pahor, N.; Mari, M.; Randaccio, L. *J. Am. Chem. Soc.* **1987**, *109*, 6045–6054.
(21) Parker, W. O., Jr.; Zangrando, E.; Bresciani-Pahor, N.; Randaccio, L.; Marzilli, L. G. *Inorg. Chem.* **1986**, *25*, 3489–3497.
(22) Parker, W. O., Jr.; Zangrando, E.; Bresciani-Pahor, N.; Marzilli, P. A.; Randaccio, L.; Marzilli, L. G. *Inorg. Chem.* **1988**, *27*, 2170–2180.
(23) Yohannes, P. G.; Bresciani-Pahor, N.; Randaccio, L.; Zangrando, E.; Marzilli, L. G. *Inorg. Chem.* **1988**, *27*, 4738–4744.
(24) Parker, W. O., Jr.; Bresciani-Pahor, N.; Zangrando, E.; Randaccio, L.; Marzilli, L. G. *Inorg. Chem.* **1985**, *24*, 3908–3913.
(25) Trogler, W. C.; Stewart, R. C.; Epps, L. A.; Marzilli, L. G. *Inorg. Chem.* **1974**, *13*, 1564–1570.
(26) Stewart, R. C.; Marzilli, L. G. *Inorg. Chem.* **1977**, *16*, 424–427.
(27) Marzilli, L. G.; Politzer, P.; Trogler, W. C.; Stewart, R. C. *Inorg. Chem.* **1975**, *14*, 2389–2393.
(28) Trogler, W. C.; Marzilli, L. G. *Inorg. Chem.* **1975**, *14*, 2942–2948.
(29) Toscano, P. J.; Marzilli, L. G. *Inorg. Chem.* **1979**, *18*, 421–424.
(30) Randaccio, L.; Bresciani-Pahor, N.; Toscano, P. J.; Marzilli, L. G. *J. Am. Chem. Soc.* **1981**, *103*, 6347–6351.
(31) Randaccio, L.; Bresciani-Pahor, N.; Orbell, J. D.; Calligaris, M.; Summers, M. F.; Snyder, B.; Toscano, P. J.; Marzilli, L. G. *Organometallics* **1985**, *4*, 469–478.
(32) Gerli, A.; Marzilli, L. G. *Inorg. Chem.* **1992**, *31*, 1152–1160.
(33) Gerli, A.; Sabat, M.; Marzilli, L. G. *J. Am. Chem. Soc.*, **1992**, *114*, 6711–6718.
(34) Pagano, T. G.; Marzilli, L. G. *Biochemistry* **1989**, *28*, 7213–7223.

Table I. ^{1}H NMR Chemical Shifts (ppm) for $[RCo(C_1py)]ClO_4$,[a] $[pyCo((DO)(DOH)pn)R]ClO_4$,[b] and $pyCo(DH)_2R$[b] Complexes in $CDCl_3$

compound	α	β[c]	γ	O–H···O	H7	NCH_2CCH_2N	$CN{=}CCH_3$	$ON{=}CCH_3$	NCCHCN
py	8.61	7.29	7.68						
2-picoline	8.49	7.08	7.56						
		7.15							
R = CH_2CF_3									
C_1py	8.16	7.13	7.68	19.00	3.69	4.43, 4.02	2.46	2.29	3.20
		7.40							
(DO)(DOH)pn	7.90	7.56	7.80	18.48		4.19, 3.77	2.53	2.37	2.22, 1.97
$(DH)_2$	8.54	7.32	7.74					2.17	
R = CH_3									
C_1py	8.31	7.14	7.65	19.30	3.62	4.36, 3.93	2.37	2.23	3.20
		7.40							
(DO)(DOH)pn	8.03	7.56	7.80	18.80		4.07, 3.79	2.45	2.30	2.08
$(DH)_2$	8.61	7.33	7.73	18.32				2.13	
R = *neo*-C_5H_{11}									
C_1py	8.25	7.10	7.63	19.59	3.61	4.37, 4.01	2.36	2.21	3.21
		7.37							
(DO)(DOH)pn	7.84	7.52	7.76	19.01		4.13, 3.66	2.48	2.34	2.25, 1.84
$(DH)_2$	8.56	7.29	7.69					2.11	
R = *i*-C_3H_7									
C_1py	8.27	7.10	7.63	19.16	3.59	4.32, 3.92	2.37	2.23	3.20
		7.38							
(DO)(DOH)pn	7.96	7.52	7.76	18.58		4.12, 3.70	2.45	2.33	2.14, 1.99
$(DH)_2$	8.60	7.28	7.70						

[a] Chemical shifts at 25 °C are relative to internal Me_4Si. [b] Data from ref 22. [c] The downfield ^{1}H resonance is for C9H; the upfield ^{1}H resonance is for C11H.

time between scans (DTBS) was 3 s, and the mixing time and 90° pulse width (PW) were 700 ms and 11.94 ms (DMSO-d_6) and 2 s and 13.6 ms (CD_3CN), respectively. The NOESY spectrum of $[BrCo(C_1py)]ClO_4$ in DMSO-d_6 resulted from a 512 × 1024 data matrix size with 16 scans (preceded by 4 DS) per t_1 value. The DTBS was 3 s, the mixing time was 2 s, and PW was 11.75 ms. A sine bell filter was used before Fourier transformation (FT) in both dimensions.

HMQC Spectroscopy.[35,36] The HMQC spectrum of $[CH_3Co(C_1py)]ClO_4$ in $CDCl_3$ resulted from a 512 × 1024 data matrix size with 64 scans (preceded by 4 DS) per t_1 value. The DTBS was 1.4 s. The HMQC spectrum of $[CH_3Co(C_1py)]ClO_4$ in DMSO-d_6 resulted from a 1024 × 2048 data matrix size with 160 scans (preceded by 4 DS) per t_1 value. The DTBS was 1 s. A 38-ms 90° PW and 63 W of ^{13}C rf power were used. A sine bell filter function was used prior to FT in the t_2 and t_1 dimensions in both cases.

HMBC Spectroscopy.[37] The HMBC spectrum of $[CH_3Co(C_1py)]ClO_4$ in $CDCl_3$ resulted from a 512 × 2048 data matrix size with 256 scans (preceded by 4 DS) per t_1 value and a DTBS of 1.4 s. In other solvents, the HMBC spectra resulted from a 1024 × 2048 data matrix size with 400 (CD_3CN) or 336 (DMSO-d_6) scans (preceded by 4 DS) per t_1 value and a DTBS of 1 s (CD_3CN) or 1.1 s (DMSO-d_6). The HMBC spectrum of $[BrCo(C_1py)]ClO_4$ in DMSO-d_6 resulted from a 512 × 1024 data matrix size with 288 scans (preceded by 4 DS) per t_1 value and a DTBS of 1.4 s. In all cases, a 38-ms 90° PW and 63 W of ^{13}C rf power were used. Values of Δ_1 (the delay between the first 90° proton pulse and the first 90° ^{13}C pulse) and Δ_2 (the delay between the first and the second 90° ^{13}C pulse) were 3.3 and 50 ms, respectively. A sine bell filter was used prior to FT in the t_2 and t_1 dimensions.

Results

Assignment of the ^{1}H NMR Spectrum of $[CH_3Co(C_1py)]ClO_4$. Two types of 2D ^{1}H–^{13}C experiments were used to unambiguously assign most of the ^{1}H signals of $[CH_3Co(C_1py)]ClO_4$ in both DMSO-d_6 and $CDCl_3$: HMQC[35,36] (^{1}H-detected heteronuclear multiple-quantum coherence) spectroscopy, which shows one-bond ^{1}H–^{13}C shift correlation; and HMBC[37] (^{1}H-detected multiple-bond heteronuclear multiple-quantum coherence) spectroscopy, which shows two- and three-bond correlations. In CD_3CN, only HMBC was used. The assignment was completed by homonuclear NOESY experiments in CD_3CN and DMSO-d_6. Shift assignments in $CDCl_3$ (Table I) for alkyl-C_1py derivatives are based on analogy with those for $[CH_3Co(C_1py)]ClO_4$. We originally selected $CDCl_3$ as a solvent for C_1py derivatives in order to compare our results with those for $(DH)_2$ and (DO)(DOH)pn derivatives (Table I). However, only alkyl-C_1py derivatives were sufficiently soluble. ^{1}H NMR spectra were acquired for all C_1py derivatives in DMSO-d_6 in order to assess chemical shift trends across a broad series; assignments (Table II) were based on the R = CH_3 2D assignments, which we now describe in detail.

The starting point for the assignment of $[CH_3Co(C_1py)]ClO_4$ in DMSO-d_6 was the three nonprotonated carbons (C2, C3, C8) of the C_1py moiety (atom-numbering in Figure 1). The three resonances (171.93, 163.00, 154.44 ppm) were recognized from the HMQC spectrum and assigned from the HMBC spectrum (Figure 2). Only the signal at 163.00 ppm shows correlations in the HMBC spectrum with the pyridine (py) protons and is then assigned to C8. The resonance at 154.44 ppm with a correlation with the oxime proton H1 in the HMBC spectrum is assigned to C2, and the remaining signal at 171.93 ppm is assigned to C3. All the observed multiple-bond ^{1}H–^{13}C connectivities are given in the supplementary material.

In the 1D ^{1}H NMR spectrum several signals are observed in the nonaromatic region. The broad multiplet at 2.93 ppm integrated for one proton is assigned to C6H. The doublet of doublets centered at 4.18 and 3.88 ppm and integrated for two protons correlate with C3 in the HMBC spectrum and therefore are assigned to nonequivalent geminal C5H′ and C5H″. In the HMBC spectrum (Figure 2), C5H′ shows a three-bond correlation to C5a (the symmetry-equivalent carbon), but C5H″ does not. Vicinal coupling constants, $^3J_{CH}$, are related to the dihedral angle, ϕ, by the Karplus equation[38]

$$^3J_{CH} = 4.26 - \cos\phi + 3.56\cos 2\phi$$

Since the halves of $[CH_3Co(C_1py)]^+$ [33] are not equivalent in the solid state, average values of ϕ were calculated. Therefore, C5H′ is the proton whose ϕ is 172° (calculated $^3J_{CH}$ of 8.7 Hz), whereas C5H″ is the proton with ϕ = 58° (calculated $^3J_{CH}$ of 2.2 Hz). As expected, C5H″ has a crosspeak to C7, but C5H′ does not (Figure 2). With two of three doublets assigned, the third at 3.47 ppm is assigned to $C7H_2$.

(35) Müller, L. *J. Am. Chem. Soc.* **1979**, *101*, 4481–4484.
(36) Bax, A.; Subramanian, S. *J. Magn. Reson.* **1986**, *67*, 565–569.
(37) Bax, A.; Summers, M. F. *J. Am. Chem. Soc.* **1986**, *108*, 2093–2094.
(38) Breitmaier, E.; Voelter, W. In *Carbon-13 NMR Spectroscopy*; VCH Publishers: New York, 1987.

Table II. ^{1}H NMR Chemical Shifts (ppm) of [R(or X)Co(C_1py)]ClO_4[a] Complexes in DMSO-d_6[b]

compound	α	β[c]	γ	O–H···H	H7	NCH_2CCH_2N	$CN{=}CCH_3$	$ON{=}CCH_3$	NCCHCN
2-picoline	8.44	7.17 7.24	7.66						
X = DMSO	7.61	7.19 7.28	7.72	18.97	3.54	4.47, 4.28	2.72	2.56	3.22
X = N_3	7.88	7.28 7.38	7.75	19.02	3.53	4.37, 4.07	2.61	2.45	3.12
X = CN	7.94	7.36 7.44	7.84	18.90	3.51	4.41, 4.06	2.52	2.35	3.08
X = Br	7.77	7.27 7.33	7.77	19.28	3.52	4.48, 4.26	2.59	2.45	3.14
X = Cl	7.80	7.25 7.33	7.75	19.24	3.53	4.42, 4.20	2.59	2.44	3.14
R = CH_2CF_3	8.12	7.34 7.42	7.81	19.19	3.50	4.25, 3.95	2.39	2.23	2.98
R = CH_3	8.25	7.34 7.43	7.79	19.40	3.47	4.18, 3.88	2.31	2.17	2.93
R = *neo*-C_5H_{11}	8.19	7.31 7.38	7.76	19.67	3.44	4.18, 3.97	2.31	2.17	2.92
R = *i*-C_3H_7	8.21	7.29 7.39	7.76	19.26	3.43	4.15, 3.88	2.33	2.19	2.90

[a] Complex with X = Cl was the PF_6^- salt. [b] Chemical shifts are relative to internal Me_4Si. [c] The downfield ^{1}H resonance is for C9H; the upfield ^{1}H resonance is for C11H.

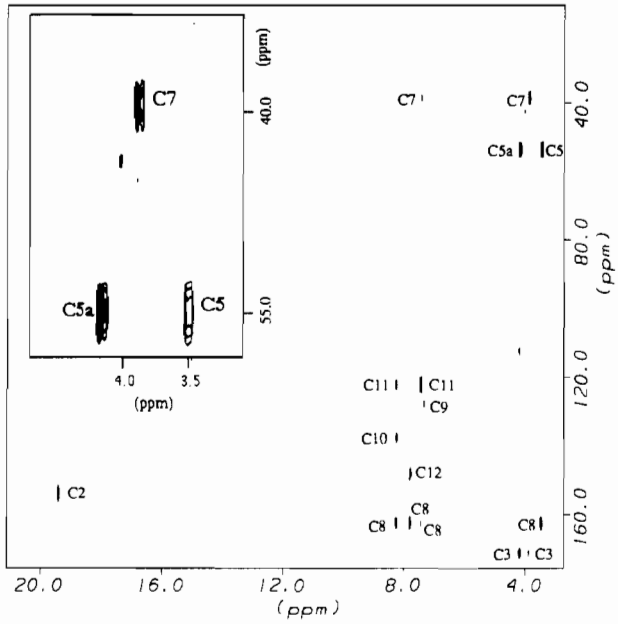

Figure 2. ^{1}H-detected ^{1}H–^{13}C multiple-bond shift correlation (HMBC) spectrum of [CH_3Co(C_1py)]ClO_4 in DMSO-d_6. Inset: C5H′, C5H″, and C7H correlations to C5a, C7, and C5, respectively.

The two sharp, upfield, intensity-6 singlets were assigned by a NOESY experiment (described below) to C4H_3 (NOE to C5H′) and to C1H_3 (NOE to H1). The intensity-3 singlet at 0.70 ppm is assigned to Co-CH_3; this signal has an NOE to H1.

The aromatic ^{1}H signals, two doublets (one for the α-H and one for C9H (β-H)) and two triplets (one for C11H (β-H) and one for the γ-H), observed for [CH_3Co(C_1py)]ClO_4 were assigned from the HMBC spectrum. The triplet at 7.79 ppm, which correlates to C8, is assigned to the γ-H, and the triplet at 7.34 ppm is assigned to C11H. C7 could be assigned as the signal at 38.18 ppm from the crosspeak with C7H_2 in the HMQC spectrum. The doublet at 7.43 ppm, which correlates to C7, is assigned to C9H. The doublet at 8.25 ppm with no correlation to C7 is assigned to C12H.

The NOESY spectrum of [CH_3Co(C_1py)]ClO_4 was used to establish through-space connectivities and to confirm the ^{1}H assignments (supplementary material). The oxime proton signal at 19.4 ppm shows NOE crosspeaks to C12H, Co-CH_3, and C1CH_3. The C5H′ signal shows NOEs to C5H″, C6H, and C4H_3. C5H″ shows NOE connectivities to C5H′ and C6H. These connectivities confirm the assignment of C5H′ and C5H″ from the HMBC spectrum. C11H shows NOEs to C10H and C12H, and C9H shows correlations to C7H and C10H. The H1–H12 NOE crosspeak confirms coordination of the pendant pyridine in [CH_3Co(C_1py)]ClO_4, *even* in DMSO-d_6.

Assignment of the ^{13}C NMR Spectrum of [CH_3Co(C_1py)]ClO_4. The ^{13}C assignments of [CH_3Co(C_1py)]ClO_4 (made by HMBC and HMQC) and those of the alkyl-C_1py derivatives, based on the 2D experiments for [CH_3Co(C_1py)]ClO_4 in $CDCl_3$ and in DMSO-d_6, are given in Tables III and IV. Shifts for analogous (DO)(DOH)pn and $(DH)_2$ derivatives are also compared in Table III.

It is interesting that all ^{1}H–^{13}C correlations observed in the HMBC spectrum for the pyridyl of [CH_3Co(C_1py)]ClO_4 (supplementary material) are those expected from the values of $^2J_{CH}$ and $^3J_{CH}$ for py itself.[38] In py, $^2J_{CH}$ is considerably enhanced when the nonbonding electron pair at nitrogen is cis to the C–H bond of the coupling hydrogen. The influence of the lone pair has been attributed to a hyperconjugative interaction: charge-transfer from the nonbonding electron pair at nitrogen to the attached HCC substructure induces a positive contribution to $^2J_{CH}$.[38]

In [CH_3Co(C_1py)]ClO_4, neither C9 nor C11 correlates to C10H, consistent with the fact that in py the Cβ–Cγ–H coupling is very small ($^2J_{CH}$ = 0.9 Hz). Correlations between C10 and C11H and between C10 and C9H are also not observed. $^2J_{CH}$ for these couplings is 0.7 Hz in py. Finally, for all the correlations we observed, the corresponding py $^2J_{CH}$ and $^3J_{CH}$ values are in the ranges 3.1–8.5 and 6.7–5.7 Hz, respectively. Thus, coordination does not significantly affect the relative values of $^2J_{CH}$ and $^3J_{CH}$ of the pyridyl of C_1py. Spectra in other solvents led to similar results and assignments.

2D NMR Studies on [BrCo(C_1py)]ClO_4 in DMSO-d_6. Assignment of the ^{1}H and ^{13}C NMR spectra in DMSO-d_6 for the non-alkyl-C_1py derivatives (Tables II and IV) was made by analogy to the [CH_3Co(C_1py)]ClO_4 assignment and confirmed with the HMBC and NOESY spectra of [BrCo(C_1py)]ClO_4. In the latter, as expected, no H1 to Co-CH_3 NOE crosspeak was observed.

A plot of the γ-^{13}C shifts (for R = CH_3, *i*-C_3H_7, *neo*-C_5H_{11}, CH_2CF_3) in $CDCl_3$ vs DMSO-d_6 gives a straight line (shift ($CDCl_3$) = −25.673 + 1.1864 × shift (DMSO-d_6), r = 0.995). With this equation and the γ-^{13}C shifts in DMSO-d_6 for non-alkyl derivatives (Table IV), we derived the corresponding shifts in $CDCl_3$ (supplementary material).

Table III. ^{13}C NMR Chemical Shifts (ppm) of $[RCo(C_1py)]ClO_4$,[a] $[pyCo((DO)(DOH)pn)R]ClO_4$,[b] and $pyCo(DH)_2R$[b] Complexes in $CDCl_3$

compound	α[c]	β[d]	γ	CN=*C	ON=*C	N*CH$_2$CH*CH$_2$N	NCH$_2$*CHCH$_2$N	C7	CN=C*CH$_3$	ON=C*CH$_3$
pyridine	149.92	123.73	135.89							
2-picoline	149.12	120.66	136.22							
	158.38	123.24								
R = CH_2CF_3										
C_1py	149.01	122.97	138.49	174.70	156.07	54.49	34.24	38.77	17.62	13.15
	163.31	129.62								
(DO)(DOH)pn	148.83	127.15	139.32	*e*	*e*	49.17	27.12		18.06	13.23
$(DH)_2$	149.94	125.42	138.03		149.94					12.22
R = CH_3										
C_1py	149.21	122.82	138.07	171.82	154.19	54.57	34.50	38.86	17.15	12.84
	162.89	128.90								
(DO)(DOH)pn	148.77	126.76	138.73	173.56	153.71	49.50	27.30		17.64	12.92
$(DH)_2$	150.06	125.21	137.48		148.98					11.98
R = *neo*-C_5H_{11}										
C_1py	148.44	122.78	137.94	171.96	155.62	54.04	34.73	39.23	17.12	12.96
	162.36	128.71								
(DO)(DOH)pn	148.00	126.71	138.51	173.99	*e*	48.71	27.09		17.66	13.01
$(DH)_2$	149.54	125.05	137.29		149.54					12.04
R = *i*-C_3H_7										
C_1py	149.21	122.68	137.91	172.00	154.57	54.09	34.62	39.58	17.10	12.91
	162.42	128.66								
(DO)(DOH)pn	148.56	122.66	138.47	*e*	*e*	48.92	27.05		17.70	12.93
$(DH)_2$	150.01	125.04	137.21		149.30					12.00

[a] Chemical shifts at 25 °C are relative to internal Me_4Si. [b] Data from ref 22. [c] The downfield ^{13}C resonance is for the substituted α-C (C8). [d] The downfield ^{13}C resonance is for C9; the upfield ^{13}C resonance is for C11. [e] Data not collected.

Table IV. ^{13}C NMR Chemical Shifts (ppm) of $[R(or\ X)Co(C_1py)]ClO_4$[a] Complexes in DMSO-d_6[b]

compound	α[c]	β[d]	γ	CN=*C	ON=*C	N*CH$_2$CH*CH$_2$N	C7	NCH$_2$*CHCH$_2$N	CN=C*CH$_3$	ON=C*CH$_3$
2-picoline	148.79	120.76	136.20							
	157.71	123.01								
X = DMSO	150.17	123.21	139.09	180.41	161.20	54.28	37.59	33.03	18.33	13.81
	165.81	130.04								
X = N_3	149.77	123.08	138.85	177.08	157.85	54.08	37.90	33.24	17.76	13.30
	165.15	129.58								
X = CN	148.23	123.27	139.01	176.76	158.11	54.63	36.99	33.23	17.66	13.24
	164.07	129.56								
X = Br	149.11	123.21	138.87	177.24	159.03	54.47	37.00	33.23	17.83	13.49
	165.03	129.82								
X = Cl	149.53	123.15	138.89	177.18	158.43	54.26	37.43	33.17	17.70	13.38
	165.21	129.67								
R = CH_2CF_3	148.52	122.77	138.35	174.64	156.57	53.55	38.17	33.59	17.09	12.76
	163.29	128.73								
R = CH_3	148.61	122.62	138.03	171.93	154.44	53.54	38.18	33.88	16.56	12.39
	163.00	128.26								
R = *neo*-C_5H_{11}	147.85	122.58	137.91	172.04	155.90	53.03	38.60	34.15	16.54	12.56
	162.38	128.01								
R = *i*-C_3H_7	148.60	122.45	137.86	172.19	154.85	53.11	38.92	34.04	16.62	12.49
	162.48	128.01								

[a] Complex with X = Cl was the PF_6^- salt. [b] Chemical shifts are relative to internal Me_4Si. [c] The downfield ^{13}C resonance is for the substituted α-C (C8). [d] The downfield ^{13}C resonance is for C9; the upfield ^{13}C resonance is for C11.

Discussion

The properties of the Co center in simple B_{12} models are of fundamental interest to the inorganic chemist. Methods of assessing the nature of the Co center have involved electrochemical, ligand dissociation, and structural studies, as well as various spectroscopic studies.[1-6] In contrast to those of cobaloximes, the redox properties of the traditional Costa-type models closely resemble those of B_{12},[32,39,40] suggesting an "electron richness" (donation of electron density from the equatorial ligand) similar to that of B_{12}.

Organo-B_{12} compounds have long axial Co–N bonds trans to the axial alkyl group.[6,11,13] Again, the traditional Costa-type complexes are better models because axial Co–N bond lengths are longer than those for cobaloximes.[21-23,32] Parallel to this property, ligand dissociation rates for B_{12} compounds are rapid[5] and such rates are somewhat faster for Costa-type than for cobaloxime complexes.[21-24]

Our interpretation of the NMR results suggested that the traditional Costa-type derivatives were, in fact, relatively electron-deficient in comparison to cobaloximes.[21,22,24] The faster rate and longer Co–N bonds could be attributed to steric interaction between the axial and equatorial ligands.[21-23] The py has orientation B in Figure 3 in Costa-type compounds and orientation A in cobaloximes. This B orientation results from steric clashes with the propylene bridge. In the C_1py derivatives, the one-methylene link forces orientation A. Bond length comparisons suggest similar properties for the Co center of $(DH)_2$ and C_1py compounds.[33] However, ligand dissociation rates cannot be measured for C_1py compounds.[33] Electrochemical studies have provided valuable information,[33] but $(DH)_2$ compounds have no charge and our C_1py and the traditional (DO)(DOH)pn models are monocationic. Electrochemical comparisons are not useful except between compounds of equal charge or in monitoring ligand-responsive trends. Therefore, we studied the ligand-

(39) Shepherd, R. E.; Zhang, S.; Dowd, P.; Choi, G.; Wilk, B.; Choi, S.-C. *Inorg. Chim. Acta* **1990**, *174*, 249–256.
(40) (a) Lexa, D.; Savéant, J.-M.; Zickler, J. *J. Am. Chem. Soc.* **1980**, *102*, 2654–2663. (b) Faure, D.; Lexa, D.; Savéant, J.-M. *J. Electroanal. Chem. Interfacial Electrochem.* **1982**, *140*, 297–309.

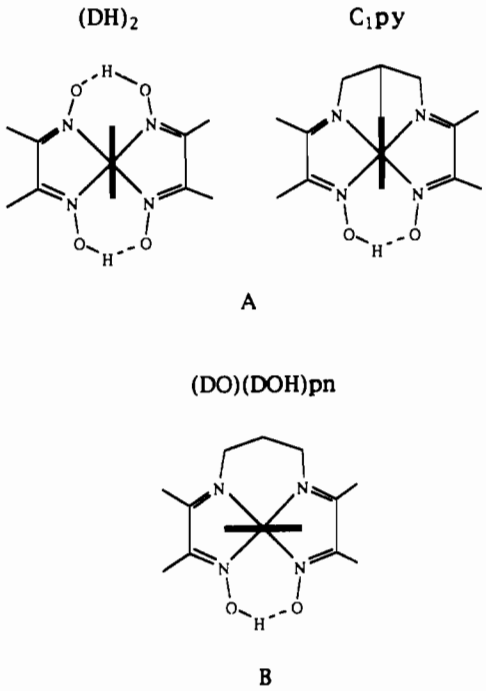

Figure 3. Eclipsed (A) and staggered (B) orientations of the py plane in C_1py, $(DH)_2$, and (DO)(DOH)pn derivatives.

responsive NMR properties of B_{12} compounds in order to assess the properties of the Co center in these new lariat complexes.

^{1}H NMR Shift Dependence on X or R. ^{1}H chemical shifts are known to be sensitive to through-space effects, such as the proximity to anisotropic groups.[5,25,27,28] In organocobalt B_{12} models, although the equatorial and axial ligands are sources of anisotropy, the main source of the anisotropy is the cobalt atom. The anisotropy of cobalt ($\Delta\chi$) generally induces upfield ^{1}H shifts of axial ligands and downfield ^{1}H shifts of the equatorial ligands as the electron-donor ability of the X or R group diminishes.[5,25] Thus, properties of the metal center can be assessed. A series must be studied, since anisotropic axial ligands influence the shifts of signals of equatorial ligand nuclei and vice versa.[25]

The anisotropic shielding effect of Co on the NMR shifts of the ligand atoms ($\Delta\sigma_{calc}$) can be approximated with McConnell's equation[41] for an axially symmetric point dipole:

$$\Delta\sigma_{calc} = (\Delta\chi)(1 - 3\cos^2\theta)/3r^3$$

where $\Delta\chi$ is the difference between the magnetic susceptibility parallel ($\chi_\parallel$) and perpendicular ($\chi_\perp$) to the dipole symmetry axis, r is the distance between Co and the observed nucleus, and θ is the angle between the vector r and the symmetry axis. The point dipole approximation is less accurate for short r values. We call $(1 - 3\cos^2\theta)/3r^3$ the geometric term (GT). The form of GT leads to a cone-shaped region of zero shielding where GT is zero at the magic angle ($\theta = 54.7°$); whether shielding or deshielding from $\Delta\chi$ occurs within or outside this cone depends on the sign of $\Delta\chi$. Thus, from $\Delta\sigma_{calc}$, changes in shifts, $\Delta\delta$, of the NMR resonances of the equatorial ligand will be opposite to those of the axial L (pyridine) ligand as the magnitude (not sign) of $\Delta\chi$ is changed by changes in the axial R or X ligand, provided the dipole symmetry axis is the (pseudo-4-fold) symmetry axis, which lies roughly along N(axial)–Co–R(or X) (Figure 1). If the dominant effect on changes in shift is the change in $\Delta\chi$, then a plot of the shift of an axial signal vs an equatorial signal will be linear with a negative slope.

Since the GT values can be calculated for complexes of known geometry, $\Delta\sigma_{calc}$ can be estimated, if a value for $\Delta\chi$ and its sign are available (see below for $\Delta\chi$ calculations). Without such

(41) McConnell, H. M. *J. Chem. Phys.* **1957**, *17*, 226–228.

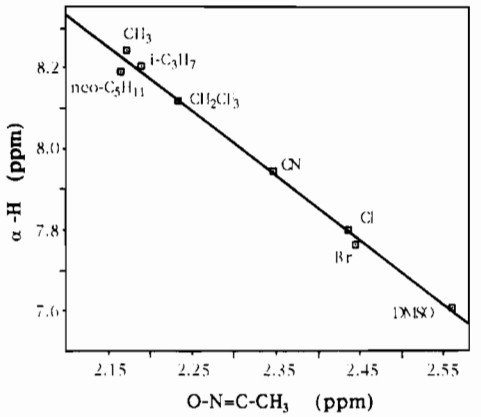

Figure 4. Plot of the ^{1}H NMR shifts of the α-H vs the ON=CCH_3 signal of $[R(or\ X)Co(C_1py)]ClO_4$ derivatives in DMSO-d_6 (for eight points (excluding N_3): s (slope) = −1.59, r (correlation coefficient) = 0.993).

detailed knowledge about $\Delta\chi$, it is still possible to deduce (a) whether or not $\Delta\chi$ is the dominant determinant of shift changes, (b) the slope in plots of δ vs δ for two ligand atoms (this slope is simply the ratio of GT values, if $\Delta\chi$ is dominant), and (c) the sign of $\Delta\chi$.

It is convenient then to define a few terms which are relative, since relative terms provide substantial information without the need to know the precise value of $\Delta\chi$. Since for the model systems both the X = Cl and the R = CH_3 derivatives are usually known and these axial ligands are nonbulky and have electron-donating ability (and hence $\Delta\chi$) near different ends of the typical series, the relative terms can best be used with reference to these derivatives.

The first useful relative term is the ligand-responsive change in shift, $\Delta\delta_{LR}$, which is a measure of the sensitivity of a given resonance for either the equatorial or L axial ligand toward changes in the X or R axial ligand, in the case of B_{12} or model systems. For X = Cl and R = CH_3, this term is specified as $\Delta\delta_{Cl-CH_3}$, i.e. $\delta_{Cl} - \delta_{CH_3}$. The second useful relative term is the ligand-responsive change in cobalt anisotropy, $\Delta(\Delta\chi)_{LR}$. This term for the two derivatives is designated as $\Delta(\Delta\chi)_{Cl-CH_3}$. From $\Delta(\Delta\chi)_{LR}$, one can calculate the ligand-responsive change in shielding, $\Delta\sigma_{LR}$ (or $\Delta\sigma_{Cl-CH_3}$ for the two derivatives). The calculated "$\Delta\delta_{LR}$" = $-\Delta\sigma_{LR}$.

The α-H shift of pyridine-type ligands is believed to be highly sensitive to $\Delta\chi$ in the cobaloxime series.[25] For t-BupyCo$(DH)_2$(R or X) derivatives, a linear relationship with negative slope (−1.6) between the α-H and the oxime CH_3 shifts was observed.[25] This value compares favorably to the slope of −2.0 calculated from the GT for the two types of protons.[25] Since the α-H shift is upfield and the oxime CH_3 shift is downfield for the Cl derivative, these observations demonstrate that (a) $\Delta\delta_{LR}$ is dominated by $\Delta(\Delta\chi)_{LR}$, (b) the sign of the $\Delta\chi$ for the Cl derivative ($(\Delta\chi)_{Cl}$) is negative, and (c) $(\Delta\chi)_{Cl}$ has the larger (more negative) value.

The same type of correlation between the α-H and the ON=CCH_3 signals observed for t-BupyCo$(DH)_2$(R or X) derivatives was found for the eight C_1py derivatives included in Figure 4 (s (slope) = −1.59; r (correlation coefficient) = 0.993). The theoretical slope is −2.3 (see below). The data point for the N_3 compound lies off the line and thus was not included: the anisotropic triatomic N_3^- ligand in $[N_3Co(C_1py)]ClO_4$ binds at an angle to the equatorial plane and affects the oxime methyl resonances. The experimental slopes are similar for the C_1py and cobaloxime models.

Similar strong correlations were found between the α-H signals and those for CN=CCH_3, NCH_2CCH_2N, and NCCHCN. In general, correlations between signals of these equatorial protons were excellent. The H7 signals in the methylene link correlated with the α-H and equatorial CH and CH_3 signals except for those of the R = i-C_3H_7 and *neo*-C_5H_{11} derivatives. The H7

Table V. ^1H and ^{13}C NMR Chemical Shifts (ppm) and Signal Assignments for Pyridine, 2-Picoline, $[CH_3Co(C_1py)]ClO_4$, $[ClCo(C_1py)]PF_6$, $[pyCo((DO)(DOH)pn)CH_3]^+$, $[pyCo((DO)(DOH)pn)Cl]PF_6$, $pyCo(DH)_2CH_3$, and $pyCo(DH)_2Cl$ in CD_3CN

			C_1py		(DO)(DOH)pn		$(DH)_2$	
	py	2-picoline	CH_3	Cl	CH_3[a]	Cl[a]	CH_3[b,c]	Cl[b,d]
C8(α)	150.71	159.36	164.13	166.27	148.24	150.63	150.06	151.04
C12(α)		150.00	150.37	151.34				
C10(γ)	136.85	137.13	138.84	139.82	138.85	140.20	137.48	138.97
C9(β)	124.72	124.00	129.31	130.86	126.07	126.72	125.21	125.67
C11(β)		121.65	123.56	124.12				
C7			39.67	38.90				
C5			54.88	55.62	49.09	49.35		
C6			35.33	34.82	26.79	27.02		
C2			155.85	159.81	154.24	158.16	148.98	152.58
C3			173.45	178.61	173.89	179.01		
C4			17.31	18.44	16.78	18.07		
C1			13.04	14.10	12.06	13.30	11.98	13.09
H8(α)	8.57				7.77	7.66	8.61	8.27
H12(α)		8.43	8.32	7.89				
H10(γ)	7.73	7.60	7.70	7.64	7.93	7.86	7.73	7.72
H9(β)	7.32	7.19	7.33	7.20	7.47	7.35	7.33	7.24
H11(β)		7.11	7.21	7.09				
C7H			3.43	3.49				
C5H′			4.12	4.34	3.72	4.17		
C5H″			3.84	4.28				
C6H			2.94	3.16	2.08	2.15		
$C4H_3$			2.23	2.53	2.39	2.60		
$C1H_3$			2.15	2.42	2.29	2.50	2.13	2.40
H1			19.46	19.32	18.99	18.79	18.32	

[a] Data from ref 32. [b] In $CDCl_3$. See Tables I and III for py shifts in $CDCl_3$. [c] Data from ref 22. [d] Data from ref 42.

Table VI. [a] Comparison between $\Delta\delta_{Cl-CH_3}$ and the Calculated Shielding $(\Delta\sigma_{Cl-CH_3})^b$ of ^1H and ^{13}C NMR Resonances in $[XCo(C_1py)]^+$, $[pyCo((DO)(DOH)pn)X]^+$, and $pyCo(DH)_2X$ (ppm)

	$[XCo(C_1py)]^+$			$[pyCo((DO)(DOH)pn)X]^+$			$pyCo(DH)_2X$		
	10^4GT[c]	$\Delta\delta_{Cl-CH_3}$	$-\Delta\sigma_{Cl-CH_3}$[b]	10^4GT	$\Delta\delta_{Cl-CH_3}$	$-\Delta\sigma_{Cl-CH_3}$	10^4GT	$\Delta\delta_{Cl-CH_3}$	$-\Delta\sigma_{Cl-CH_3}$
H12(α)	−73.5	−0.43	−0.49	−84	−0.11	−0.58	−71	−0.34	−0.49
H9(β)	−42	−0.12	−0.29	−41	−0.12	−0.28	−36	−0.09	−0.25
H11(β)	−44	−0.13	−0.29						
H10(γ)	−36	−0.06	−0.24	−36	−0.07	−0.24	−32	−0.01	−0.22
$C7H_2$	−14.5	0.06	−0.10						
$C4H_3$	32	0.30	0.22	32	0.21	0.22	30	0.27	0.21
$C1H_3$	32	0.27	0.21	32	0.21	0.22			
C5H′	56	0.25	0.38	60	0.45	0.40			
C5H″	66	0.42	0.46						
$C6H_2$	38.5	0.22	0.26	36	0.07	0.24			
H1	171	−0.14	1.15	196	−0.20	1.32			
C8(α)	−206	2.14	−1.38	−203	2.39	−1.37	−192	0.98	−1.33
C12(α)	−213	0.97	−1.43						
C11(β)	−78	0.56	−0.52	−79	0.65	−0.50	−74	0.46	−0.51
C9(β)	−81	1.55	−0.54						
C10(γ)	−63	0.98	−0.43	−62	1.35	−0.42	−59	1.49	−0.41
C7	−28	−0.77	−0.19						
C1	45	1.06	0.30	45	1.24	0.30	45	1.11	0.31
C4	45	1.11	0.30	45	1.29	0.30			
C2	160	3.96	1.07	161	3.92	1.08	160	3.60	1.10
C3	163	5.16	1.10	163	5.12	1.09			
C5	130	0.74	0.87	128	0.26	0.86			
C6	89	−0.71	0.60	89	0.41	0.60			

[a] Crystallographic data obtained from refs 24, 32, 33, and 43; NMR data from Table V. [b] $\Delta\sigma_{Cl-CH_3} = GT \times \Delta(\Delta\chi)_{Cl-CH_3}$; calculated from the average of the $\Delta\chi_{LR}$ bold values in Table VII. Note that the calculated difference in shielding "$\Delta\delta_{Cl-CH_3}$" is $-\Delta\sigma_{Cl-CH_3}$. [c] $GT = (1 - 3\cos^2\theta)/3r^3$ (in $Å^{-3}$).

signals for the two derivatives were shifted too far upfield to correlate well. As found previously for cobaloximes, the γ-H and β-H ligand-responsive trends were similar, but the shifts did not correlate with the α-H or equatorial ^1H signals. No trends in the oxime H signal were evident.

The pyridine moiety in both $(DH)_2$ and C_1py derivatives lies over the Co–N–O—H···O–N chelate rings, and in both cases the α-H shifts are presumably not greatly subject to the anisotropy of the equatorial C=N double bonds. The upfield coordination shift of the α-H of $[ClCo(C_1py)]^+$ relative to the α-H shift in free 2-picoline is greater than the upfield coordination shift observed for the α-H of $pyCo(DH)_2Cl$[42] (Tables I and V). This α-H upfield coordination shift is largest for $[pyCo((DO)(DOH)pn)Cl]^+$.[32] However, the GT's ($\times 10^4$ $Å^{-3}$) for the α-H (−70 to −84) and equatorial CH_3's (~30) are fairly similar in all three model systems, if the point dipole symmetry axis is assumed to lie directly along the Co–N(axial) bond (see Table VI). The ratio of GT values for $[ClCo(C_1py)]^+$ is −2.3. The GT values were calculated from the X-ray structures of the Cl derivative[32,33] except those for the cobaloxime, where only the methyl structure[43] has been reported. However, the GT value is not very dependent on the axial ligand and differs by less than 10% for axial ligands and

(42) Toscano, P. J. Personal communication.

5% for equatorial ligands. Our goal here, since the $\Delta\chi$ value cannot be determined accurately in solution, is to identify the dominant factors influencing the ligand-responsive trends.

For the equatorial CH_3, $\Delta\delta_{Cl-CH_3}$ is 0.27 ppm for py/$(DH)_2$ and 0.27–0.30 ppm for C_1py compounds (Table VI). For the α-H, $\Delta\delta_{Cl-CH_3}$ is higher for C_1py (–0.43 ppm) than for py/$(DH)_2$ (–0.34 ppm) compounds. Therefore, on the basis of the α-H and equatorial CH_3 signals, ligand-responsive changes in cobalt anisotropy $\Delta(\Delta\chi_{LR})$ and probably $\Delta\chi$ itself are perhaps slightly greater for C_1py than for $(DH)_2$ compounds.

The py α-H resonance in (DO)(DOH)pn derivatives in $CDCl_3$ is upfield from that of analogous $(DH)_2$ derivatives (Table I). Since the py in (DO)(DOH)pn derivatives is oriented with the two α-H's lying over the equatorial C=N double bonds (Figure 3),[24] it has been suggested that the resonance of the α-H's can be influenced in part by the proximity of these protons to the equatorial anisotropic ligand.[23,24] Since this conclusion was based on comparison of Costa-type complexes with cobaloximes, conceivably, the charge differences could have influenced the shift.

To assess this effect, comparison of the similarly charged C_1py and (DO)(DOH)pn derivatives is extremely useful: the equatorial ligands are very similar,[33] the only major difference being the pyridine orientation (Figure 3). $\Delta\delta_{Cl-CH_3}$ for the α-H signal is only ~–0.1 ppm for (DO)(DOH)pn, compared to ~–0.4 ppm for both C_1py and cobaloxime models. The α-H upfield shift in C_1py complexes relative to free 2-picoline is much smaller than the py α-H upfield shift observed for (DO)(DOH)pn derivatives relative to free py in both $CDCl_3$ and CD_3CN (Tables I and V). We concluded previously[21,23,24] that a significant part of the py α-H shielding in (DO)(DOH)pn derivatives arises from the proximity of the two α-H's to the anisotropic five-membered Co–N–C–C–N rings. The charge difference is not important. This interpretation gains further support from the larger α-H coordination shifts found for (DO)(DOH)Me_2pn than for (DO)-(DOH)pn compounds.[23]

The equatorial ligand anisotropy confounds the comparison of Co anisotropy in C_1py with (DO)(DOH)pn compounds using the α-H shifts. The situation is somewhat clearer for the equatorial CH_3 signals. The greater anisotropy of the X = Cl derivative should shift these CH_3 signals downfield relative to those of the R = CH_3 derivative, as found. The effect is greater for C_1py than for (DO)(DOH)pn compounds (Table VI). A similar effect should be observed for the methyl C signals, but these are shifted more downfield in (DO)(DOH)pn. Likewise, the py C's are somewhat less downfield shifted in the Cl relative to CH_3 derivative of C_1py. Thus, most of the indications suggest somewhat greater $\Delta(\Delta\chi_{LR})$ for the Co center in C_1py than in (DO)(DOH)pn compounds, although no individual result is compelling.

In contrast to the much smaller $\Delta\delta_{LR}$ for the α-H of (DO)(DOH)pn than of C_1py compounds, the β-H and γ-H $\Delta\delta_{LR}$ in both these Costa-type models are similar (Table VI). This finding provides *very strong evidence* that the α-H shift in (DO)-(DOH)pn is greatly influenced by the equatorial ligand anisotropy, since this anisotropy will affect the α-H shifts primarily. The other two factors influencing shift, Co anisotropy and inductive effects, are similar in these two systems, as suggested by the size of $\Delta\delta_{Cl-CH_3}$ for the β- and γ-H signals (Table VI). Thus, these signals lead to the conclusion that the $\Delta(\Delta\chi)_{Cl-CH_3}$ for the C_1py compounds is not larger than in traditional Costa-type compounds. However, inductive effects need to be analyzed since these are important for the β- and γ-H signals.

Above we stated that (a) the α-H and equatorial CH_3 signals generally correlated, (b) the experimental slope for this correlation was too low compared to the theoretical, and (c) the β-H and γ-H shifts did not correlate very well. Relatively simple cobaloximes were used to develop the concept that Co anisotropy dominates ^{1}H $\Delta\delta_{LR}$.[25] Complicating matters, the relatively low-field instruments available made measurements of small β-H $\Delta\delta_{LR}$ difficult and the low sensitivity required use of more soluble *t*-Bupy/$(DH)_2$ derivatives, which lack a γ-H. The agreement of the α-H vs CH_3 slope with theory seemed acceptable, especially since the dipolar relationship is not expected to be very good for close-in nuclei because Co is not a point dipole.[25]

Table VII. Ligand-Responsive Change in Cobalt Anisotropy $(\Delta(\Delta\chi)_{Cl-CH_3})$ for C_1py, py/(DO)(DOH)pn, and py/$(DH)_2$ Cobalt Complexes[a]

	$\Delta(\Delta\chi)_{Cl-CH_3}$		
	$(DH)_2$	C_1py	(DO)(DOH)pn
α-H(av)	**–48**	**–58**	–13
C3H_3(av)		–94	–65
C1H_3(av)		–84	–65
CH_3(av)	**–91**	**–89**	**–65**
C5H′(av)		–45	–69
C5H″(av)		–61	
C6H		–57	–19[b]
C5H_2,C6H(av)		**–54**	**–69**
α-H(av)/CH_3(av)[c]	**–69**	**–73.5**	
average in bold[d]	**–69**	**–67**	**–67**

[a] Units are cm^3/molecule; values in table are multiplied by 10^{30}. [b] Not considered for the average since signals are complex multiplets obscured by methyl signals. [c] Average of bold α-H(av) and CH_3(av) only. [d] Average of all numbers in bold.

Compared to $(DH)_2$ compounds, the C_1py compounds have many more "reporter" protons distributed throughout the molecule. The observation for these two series that the axial vs equatorial slope is less than theoretical has several possible explanations: (a) the ligand-responsive α-H shift is too small, (b) that for equatorial CH_3 is too large, and (c) both (a) and (b) occur. Alternatively, the low slope could be due to the deficiency in the point dipole approximation. However, the observed $\Delta\delta_{Cl-CH_3}$ is even lower than expected for the β-H's and the γ-H (Table VI). This suggests that the ^{1}H $\Delta\delta_{LR}$ are also influenced by inductive effects which must oppose $\Delta(\Delta\chi_{LR})$ in the axial direction and must augment $\Delta(\Delta\chi_{LR})$ in the equatorial direction. The GT term suggests that Co anisotropy should shift C7H upfield, whereas it actually shifts downfield. This finding is also consistent with an inductive effect. Since the donation by the pyridyl is greater in C_1py than in (DO)(DOH)pn compounds, there is a greater inductive (downfield shifting) effect on the py ^{1}H signals. Thus, the upfield shift of the β- and γ-H's is lower than expected from the greater $\Delta(\Delta\chi_{LR})$ of the C_1py compounds suggested by the greater $\Delta\delta_{LR}$ of methyl ^{1}H signals.

For the reasons just given, $\Delta(\Delta\chi)_{Cl-CH_3}$ was estimated by excluding the γ-H, β-H, and H7 shifts, by assuming no inductive effects for either compound, and by using an average of $\Delta(\Delta\chi)$ calculated from other shifts (Table VII). For $[ClCo(C_1py)]^+$, this approximation gave a value for $\Delta(\Delta\chi)_{Cl-CH_3}$ of -6.7×10^{-29} cm^3/molecule. From a similar estimate for $pyCo(DH)_2Cl$, we would assign a value of -6.9×10^{-29} cm^3/molecule. If $\Delta(\Delta\chi)_{Cl-CH_3}$ values from the α-H and average equatorial CH_3 signals are averaged, the resulting value of -7.4×10^{-29} cm^3/molecule for $[ClCo(C_1py)]^+$ exceeds that for $pyCo(DH)_2Cl$ somewhat, as also assessed qualitatively above.

It should be noted that, in the absence of an unlikely sign change in $\Delta\chi$, a more accurate estimate of $\Delta(\Delta\chi)_{Cl-CH_3}$ can be made, if the size of the contribution to $\Delta\delta_{LR}$ of inductive effects is known. Attempts have been made to estimate this contribution for axial ^{13}C shifts.[16] For axial ^{1}H shifts, this correction is relatively small since the shifts for the alkyl complexes are very similar to those for the free ligand; i.e., on coordination the shifts for the α-H are small (0.2 ppm for CH_3 vs 0.6 ppm for Cl). Thus, a ~33% underestimate of $\Delta(\Delta\chi)_{Cl-CH_3}$ using the α-H shift is introduced by ignoring inductive effects. There is no simple way to estimate the error in $\Delta(\Delta\chi)_{Cl-CH_3}$ introduced by inductive effects

(43) Bigotto, A.; Zangrando, E.; Randaccio, L. *J. Chem. Soc., Dalton Trans.* **1976**, 96–104.

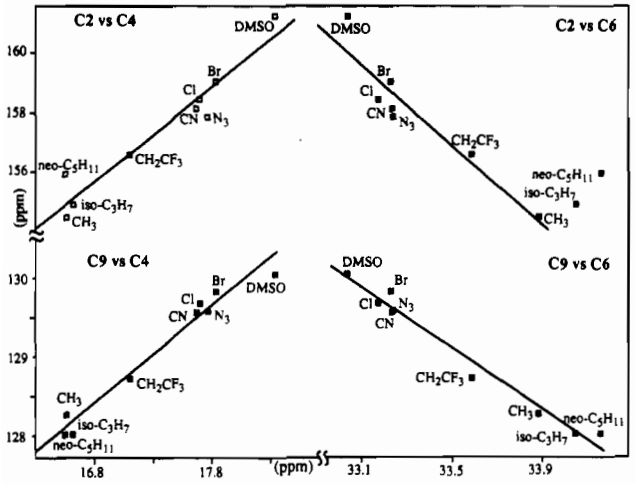

Figure 5. Plots of the ^{13}C NMR shifts of $[R(or\ X)Co(C_1py)]ClO_4$ derivatives in DMSO-d_6 for the β-C (C9) vs C4 and C6 (for nine points: $s = 1.23$, $r = 0.968$ for C4; $s = -1.93$, $r = 0.975$ for C6) and plots of the ^{13}C NMR shifts of C2 vs C6 and C4 (for C6, without the *neo*-C_5H_{11} and *i*-C_3H_7 points, $s = -6.77$, $r = 0.888$; for C4, $s = 3.16$, $r = 0.927$).

for the equatorial ligands, since the "free" ligands do not exist in these solvents. However, $\Delta(\Delta\chi)_{Cl-CH_3}$ based on the equatorial methyl signals will be *overestimated*, if no correction is made for inductive effects. Thus, an average $\Delta(\Delta\chi)_{Cl-CH_3}$ from axial and equatorial shifts (Table VII) is probably reasonable and more than adequate for our purposes. We used the "average in bold" values (Table VII) to calculate $-\Delta\sigma_{Cl-CH_3}$ in Table VI.

The inductive effect and the anisotropy are larger for the chloro complexes. For $[ClCo(C_1py)]^+$, $(\Delta\chi)_{Cl}$ can be *crudely* estimated to be $\sim\Delta(\Delta\chi)_{Cl-CH_3}$ by recognizing that for the CH_3 derivative (a) the anisotropy and (b) the inductive effect are small.

The downfield shift of the O–H···O signal in C_1py derivatives with respect to those in analogous cobaloximes and (DO)(DOH)-pn derivatives (Tables I and V) could reflect stronger H bonding in the C_1py derivatives. Both anisotropic and inductive arguments suggest that the signals of the Cl derivatives should be downfield from those of the CH_3 derivative. This wrong-way ligand-responsive shift for H1 between the Cl/CH_3 Costa-type derivatives probably does not reflect anisotropy of the pyridine ring because it has different orientations in the models (Figure 3).

^{13}C NMR Shift Dependence on X or R. In contrast to trends in ^1H NMR chemical shifts, for cobaloximes it has been found that ^{13}C resonances of both equatorial and axial ligands move downfield as the electron-donating ability of X is decreased.[5] The $\Delta\delta_{LR}$ of ^{13}C resonances are influenced relatively little by anisotropic effects, since $\Delta(\Delta\chi)_{LR}$ effects are small compared to the relatively large $\Delta\delta_{LR}$ of ^{13}C signals.[26]

In Table VI, we compare observed shift changes, $\Delta\delta_{Cl-CH_3}$, with $-\Delta\sigma_{calc}$. It is clear that the observed differences are usually much larger than the calculated effect of $\Delta(\Delta\chi)_{LR}$, consistent with the previous conclusion that Co anisotropy effects on ^{13}C signals are in general small compared to inductive effects.[26] This conclusion would not change even if the anisotropy were twice that estimated above, an unlikely possibility since the sources of error considered above are not that large.

The good linear correlation ($s = 1.23$, $r = 0.968$) between C9 (the β-C) and C4 (Figure 5) can be attributed to inductive effects, primarily. As the electron-donor ability of R(or X) diminishes (on going from *neo*-C_5H_{11} to DMSO), there is a downfield shift of the ^{13}C resonances of C9. This is consistent with increased donation by the pyridine moiety. Good positive correlations were obtained between C9 and the five-membered chelate ring carbons (C1, C2, and C3). A good positive correlation was found between C9 and the γ-C (C10). Likewise, C10 shifts were compared with those of equatorial C's (C1–C6). The slopes with C1–C5 were positive and that with C6 was negative, but the correlations were not as good as with C9. A principal cause for these poorer correlations could be the X = CN C10 shift due to the unusual properties of the CN ligand noted previously.[26] The participation of CN^- in π-bonding in cobaloximes has been reported recently.[44]

The better correlation for C4 for both C9 and C10 reflects deviations for the C1, C2, and C3 points for R = *i*-C_3H_7 and *neo*-C_5H_{11}. These deviations could be due to the bulk of these two alkyl groups, which could force them to lie close to C1 and C2 and away from C4. In the X-ray structure of [pyCo((DO)-(DOH)pn)-*neo*-C_5H_{11}]PF_6,[24] the neopentyl group indeed lies in this region. This interpretation can also explain the unusual oxime H-shift of [*neo*-$C_5H_{11}Co(C_1py)]ClO_4$ (the most downfield of any alkyl-C_1py compound).

Correlations between C1, C2, C3, and C4 shifts are generally good, with positive slopes. Correlations for these C's with C6 are somewhat poorer (Figure 5).

In general, C5, C7, C11, and C12 gave relatively poor correlations, with correlations involving C8 generally not quite so poor. Previously, we found that α-C's give poor correlations.[26] The C5 and C7 signals are probably affected by both steric and inductive effects, explaining the poor results. We believe that C11 correlates poorly because its shift range is small and ligand-responsive trends may be masked by other factors such as solvent effects.

As mentioned above, the shifts (and hence binding) in cyano-B_{12} model complexes can be anomalous.[44] The somewhat better correlations for C8 reflect the midranking of CN for this signal. The CN point varies considerably, often being the extreme downfield shift for a given C (C11, C7, C5) but sometimes being close to the most upfield shift (C12). Thus, C5 and C11 usually have poor correlations, but they correlate reasonably well with each other.

The most surprising correlation to emerge was that between C9 and C6 ($s = -1.93$, $r = 0.975$) (Figure 5), since there is an upfield shift of ^{13}C resonances of the equatorial C6 for the weaker axial ligands. Furthermore, the signals for the carbons bound to C6 (C5 and C7) show poor correlations with C9. The C6 $\Delta\delta_{LR}$ is in the opposite direction than that expected if inductive effects would dominate. Furthermore, the observed trend cannot be explained in terms of $\Delta\chi$, which should induce a downfield shift for C6 as the electron-donor ability of R(or X) diminishes. The GT has a positive sign. For C_1py CH_3 vs Cl derivatives in CD_3-CN, an *upfield* shift of 0.71 ppm was found vs a *downfield* shift of 0.41 ppm for the (DO)(DOH)pn analogs (Table VI). A possible explanation of the upfield shift of C6 for the weaker electron-donor axial ligands is that the shift is influenced by strain. Upon a decrease in the electron-donor ability of R(or X), the Co–N(axial) bond distance decreases.[5] Since the pyridyl moiety in C_1py derivatives is connected through a one-methylene link to C6, Co–N(axial) bond distance variations might slightly affect bond and torsion angles at C6. The pattern between C6 and C9 was also observed with the other pyridine carbons, although the correlations were not so good as that involving C9.

The C1–C4 signals probably sense the average electron density on Co. As the axial ligand becomes a better donor and becomes bulkier (CH_3 vs *neo*-C_5H_{11} and *i*-C_3H_7), the increased donation by R may be offset by decreased donation by the pyridyl group. The net effect on the equatorial C signals may be small. The C3 and C4 shifts are similar for derivatives with these three alkyl groups. The $\Delta\delta_{LR}$ of the C1 and C2 signals actually suggest that the bulkier alkyls are worse donors than CH_3, whereas the $\Delta\delta_{LR}$ for the axial C signals C7–C12 suggest the opposite conclusion.

The C6 vs equatorial C1–C4 shifts clearly indicate a large steric effect for the *neo*-C_5H_{11} and *i*-C_3H_7 groups (Figure 5). The C6 and adjacent C7 have signals which generally shift downfield as X or R donor ability increases. For C7, *i*-C_3H_7 has the larger effect; in contrast, for C6, *neo*-C_5H_{11} has the larger effect. Both

(44) Brown, K. L.; Satyanarayana, S. *Inorg. Chem.* **1992**, *31*, 1366–1369.

bulky alkyl groups induce similar upfield shifts in H7. Thus, steric effects for these bulky groups are clearly evident in some signals.

Relative to 2-picoline, the γ-C signal is downfield in C_1py derivatives, as expected from electron donation from the pyridyl moiety to Co. The ^{13}C NMR shift of the γ-C in C_1py derivatives moves downfield across the series as the electron-donor power of the alkyl group is decreased (supplementary material), consistent with the expected increased donation by the pyridine. Furthermore, the shifts of the pyridine γ-C's are influenced in relatively the same manner in the three model systems. This is evidenced by good linear relationships between the γ-^{13}C chemical shifts of $[R(\text{or X})Co(C_1py)]ClO_4$ complexes and analogous (a) [pyCo((DO)(DOH)pn)R]ClO_4, (b) *t*-BupyCo$(DH)_2$R(or X) (*t*-Bupy = 4-*tert*-butylpyridine), and (c) pyCo$(DH)_2$R(or X) complexes (supplementary material). The anomalous effect of CN is manifested in the same manner in $(DH)_2$ as in C_1py derivatives.

For a given R derivative, the average downfield shift for both β-C's and the γ-C, relative to the appropriate free ligand, follows the order C_1py > (DO)(DOH)pn ≫ $(DH)_2$. We attribute the greater effect in C_1py to the shorter Co–N(axial) distance in C_1py derivatives, which leads to an increase in electron donation from the pyridine moiety to Co. The greater difficulty in reducing C_1py compared to (DO)(DOH)pn Co(III) derivatives is another consequence of this donation.[33]

Electrochemical Correlations. The redox properties of C_1py neopentyl and isopropyl derivatives are unusual.[33] If one assumes that these groups are better donors than methyl, the E_{pc} or $E_{1/2}$ values for derivatives with bulky alkyls should be more negative than for the methyl derivative ($E_{1/2} = (E_{pc} + E_{pa})/2$, experimental approximation of the standard potential of a redox couple; E_{pc} and E_{pa}, cathodic and anodic peak potentials). However, this is not the case. There are two obvious explanations: First,[39] the bulk of the alkyl could decrease the electron donation since the Co–C bond is long; the good relationship cited above between the redox properties of the C_1py model[33] and cobalamins[39,40] would then suggest a similar steric/electronic effect, although the *i*-C_3H_7 cobalamin redox properties are not known. Second, the redox process could reflect Co–C bond cleavage, which occurs after reduction. The following chemical reaction would be reflected in E_{pc} ($E_{1/2}$), and consequently the faster rate of homolysis of the bulkier alkyls could account for the observed trend. Again, the similarity of C_1py and cobalamins could mean that the relative rate of cleavage would be similar.

The ^1H and ^{13}C shift trends, especially the latter, should not necessarily follow the homolysis rate (second explanation), but should be reflected by E_{pc} values if the first explanation holds. Therefore, it is of some interest to examine more closely the correlation between E_{pc} (and $E_{1/2}$) and ligand-responsive shifts.

There are some good correlations (in all cases for nine points) between E_{pc} and the α-H (H12) ($r = 0.973$), $C1H_3$ ($r = 0.960$), and $C4H_3$ ($r = 0.946$) shifts and reasonable correlations for H6 ($r = 0.941$), H5′ ($r = 0.826$), and H5″ ($r = 0.891$). This suggests that $\Delta\delta_{LR}$ reflects the net electron richness of the Co center and that the electron donation by the bulky alkyls is compensating somewhat for the lower donation by the pyridyl moiety. The comparison of solvato species involves DMSO (for NMR) and CH_3CN (for E_{pc}) as axial ligands. Furthermore, the charge of these species is 2+ vs 1+ for the other derivatives. If the solvato point is excluded, these correlations generally improve. The correlation of H7, a signal that appears to reflect steric factors influencing pyridyl donation, with E_{pc} is poor.

The axial ^1H shifts that reflect pyridyl donation correlate with E_{pc} poorly for H9 ($r = 0.688$), H10 ($r = 0.274$), and H11 ($r = 0.655$), all for nine points. The bulky alkyl shifts are too far upfield, and the CN shifts are too far downfield. If these points are removed, the correlations (for six points) improve: H9 ($r = 0.938$), H10 ($r = 0.896$), and H11 ($r = 0.969$).

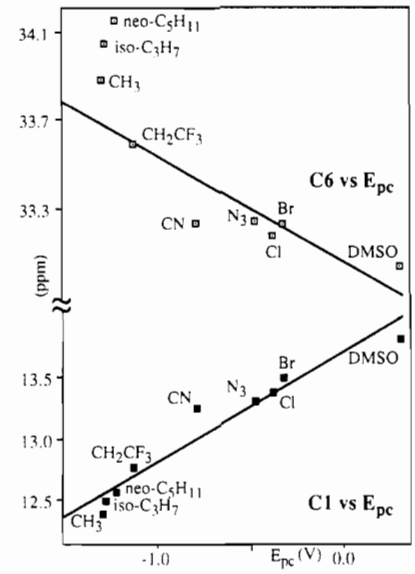

Figure 6. Plots of the ^{13}C NMR shifts of C1 and C6 (in DMSO-d_6) vs E_{pc} (in CH_3CN) for $[R(\text{or X})Co(C_1py)]ClO_4$ derivatives (for nine points, $s = 0.89$, $r = 0.935$ for C1; the line is drawn (for seven points) without the *neo*-C_5H_{11} and *i*-C_3H_7 points for C6 ($s = -0.48$, $r = 0.795$)).

From the better correlations only, it appears that the solvato potential is too positive, but also that the CN potential is too negative. This is true regardless of the sign of $\Delta\delta_{LR}$. If only these two points are excluded, the correlations with E_{pc} are (for seven points) $r = 0.990$ for H12, $r = 0.980$ for $C1H_3$, $r = 0.971$ for $C4H_3$, $r = 0.982$ for H6, and $r = 0.965$ for H5′.

This CN/DMSO trend is even more evident in the ^{13}C results. The correlations (for R = *neo*-C_5H_{11}, *i*-C_3H_7, CH_3, CH_2CF_3 and X = CN, N_3, Br, Cl, DMSO) between E_{pc} and the equatorial carbons (C1–C4) are better than those between E_{pc} and the axial C's (C7–C12). We find (for nine points) very good to fairly good correlations between E_{pc} and C1 ($r = 0.935$) (Figure 6), C2 ($r = 0.925$), C3 ($r = 0.918$), and C4 ($r = 0.903$) shifts and poor correlations between E_{pc} and the β- and γ-C's (C9–C11), which respond to the nature of the axial ligand ($r = 0.836$ for C9, $r = 0.754$ for C10, and $r = 0.680$ for C11).

If CN and DMSO points are excluded (for the reasons discussed above), the correlations between E_{pc} and the ^{13}C shifts improve (especially C9, C10, and C11), except those for C2 and C12. Correlations (for seven points) for the equatorial C1–C4 and β- and γ-C's follow: $r = 0.983$ for C1, $r = 0.909$ for C2, $r = 0.928$ for C3, $r = 0.946$ for C4, $r = 0.951$ for C9, $r = 0.932$ for C10, $r = 0.944$ for C11.

The greater ease of reduction of the solvato complex vs that expected from the ^1H and ^{13}C shifts can be attributed to overall charge. The reason for the difficulty in reducing the CN compound is less clear. Apparently, the CN ligand is relatively more capable of stabilizing the higher Co^{III} oxidation state than it is capable of donating charge to the Co^{III}.

In contrast to the effect of removing the CN and DMSO points, removal of the neopentyl and isopropyl points in general causes a small decrease in r. However, only seven points are in the correlation and the decrease is therefore real. This result implies that the electronic properties of the Co center are reflected in both E_{pc} and ^{13}C shifts. For two signals, C6 and C8, the r value increased. The correlations ($r = 0.767$ for C6 and $r = 0.908$ for C8 for nine points) improve ($r = 0.795$ for C6 and $r = 0.927$ for C8 for seven points). However, the C8 signal must be responding to several effects (anisotropy, inductive effects, and strain) and is difficult to assess. The C6 signal correlates poorly with E_{pc} (Figure 6). We feel that this signal reflects only the steric changes in the complex.

In summary, regardless of whether or not CN and DMSO points are excluded, the E_{pc} values appear to closely reflect total

electron donation to the Co center as assessed by either ^1H or ^{13}C shifts. The steric effects of the bulky alkyl groups are manifest in some signals, particularly C6; this result indicates that pyridyl is consequently a weaker donor. E_{pc} does not appear to be as sensitive to steric effects because the bulky R groups are better donors and increase the electron richness of the Co center.

Conclusions

In C_1py derivatives the pyridyl moiety is anchored to the equatorial ligand, and it occupies a somewhat fixed position. Therefore, it is possible to assess the relative contribution of anisotropic and electronic effects on the ^1H and ^{13}C NMR shifts of the pendant pyridine. The situation contrasts that found in (DO)(DOH)pn derivatives, for which rotation of the pyridine around the Co–N bond did not allow such assessment.

^1H NMR shifts of C_1py derivatives appear to be greatly influenced by anisotropy of cobalt as shown by good correlation with *negative* slope between axial and equatorial proton resonances. On the basis of equatorial methyl ^1H shifts, the $\Delta(\Delta\chi_{LR})$ for the three model systems analyzed in this work are very similar and dominate ^1H $\Delta\delta_{LR}$. The greater shielding of the pyridine α-H signal in (DO)(DOH)pn derivatives compared to C_1py and $(DH)_2$ derivatives is therefore due to anisotropy of the equatorial ligand.

On the contrary, $\Delta\delta_{LR}$ for most pyridine ^{13}C resonances, ^{13}C resonances of the equatorial carbons that are part of the conjugated system, and ^{13}C resonances of carbons directly connected to and coplanar with the unsaturated system (C1 and C4) shift downfield as the electron-donor ability of R(or X) is decreased. These ^{13}C shifts correlate with a *positive* slope. Thus, most of these ^{13}C $\Delta\delta_{LR}$ are particularly sensitive to through-bond inductive effects and not to $\Delta(\Delta\chi_{LR})$. The pyridyl β- and γ-C signals respond to the nature of the axial ligand, including potential π-bonding in the CN ligand.[44]

As the electron-donor ability of R(or X) diminishes, there is an upfield shift of C6, the carbon of the equatorial ligand that is the point of attachment of the pendant pyridine. This C6 upfield shift and a less smooth shift for C7 can be explained in terms of conformational strain imposed by a decrease in the Co–N(axial) bond distance. Thus, this C6 ^{13}C $\Delta\delta_{LR}$ in these C_1py model compounds appears to reflect the $\Delta\delta_{LR}$ trend found with ^{31}P shifts in B_{12} compounds.[13]

Comparison of ^{13}C data suggests that there is greater electron donation of the pyridine moiety to Co in C_1py compared to (DO)(DOH)pn and $(DH)_2$ derivatives. We attribute these results to the greater electron richness of the $(DH)_2$ system and to the different pyridine orientation in C_1py and (DO)(DOH)pn derivatives that allows a shorter Co–N(axial) distance in C_1py derivatives.

There are good correlations between E_{pc} and shifts. However, different classes of signals provide insight into structural and electronic changes in different parts of the molecule. For some signals, such as C3 and C4, these comparisons suggest that the E_{pc} reflects the overall electron donation. Thus, although modulation of E_{pc} by the following chemical reactions (i.e. homolysis of the Co(III)–C bond) cannot be excluded, the primary cause for the less negative E_{pc} value for both C_1py and B_{12} derivatives with bulky electron-donating alkyl groups probably is the compensating weaker donation by the N axial ligand.

Acknowledgment. We are grateful to the National Institutes of Health (Grant GM 29225) for financial support. We thank Dr. Hoshik Won for writing the program that calculates GT from crystallographic results and M. Iwamoto for performing some of the 500-MHz NMR experiments.

Supplementary Material Available: Tables of the observed HMBC and NOESY connectivities in $[CH_3Co(C_1py)]ClO_4$ and of the γ-^{13}C NMR shifts for $[R(orX)Co(C_1py)]ClO_4$, *t*-Bupy(or py)$Co(DH)_2R$(or X), and $[pyCo((DO)(DOH)pn)R]ClO_4$ complexes in $CDCl_3$, HMQC spectrum, NOESY spectrum, and expanded region of the NOESY spectrum of $[CH_3Co(C_1py)]ClO_4$ in DMSO-d_6, plots of the γ-C ^{13}C NMR shifts (in $CDCl_3$) of $[RCo(C_1py)]ClO_4$ vs $[pyCo((DO)(DOH)pn)R]ClO_4$ derivatives, of $[R(or X)Co(C_1py)]ClO_4$ vs *t*-Bupy$Co(DH)_2R$(or X) derivatives, and of $[R(or X)Co(C_1py)]ClO_4$ vs $pyCo(DH)_2R$(or X) derivatives, and a plot of ^1H NMR shifts (in DMSO-d_6) of the α-H vs E_{pc} (in CD_3CN) of $[R(or X)Co(C_1py)]ClO_4$ derivatives (10 pages). Ordering information is given on any current masthead page.